

## Monitoring Crustal Deformation in Satakunta Region

Sonja Nyberg<sup>1</sup>, Markku Poutanen<sup>1</sup>, Ulla Kallio<sup>1</sup> and Joel Ahola<sup>2</sup>

<sup>1</sup>Finnish Geodetic Institute, Geodeetinrinne 2, 02430 Masala, Finland

<sup>2</sup>Espoo, Finland

(Received: April 2010; Accepted: July 2010)

### *Abstract*

*The GeoSatakunta GPS network was established in 2003 to obtain information on contemporary crustal deformations in the Satakunta region. The network consists of 13 concrete pillars for episodic GPS campaigns and the Olkiluoto permanent GPS station. The baseline lengths range from five to 65 km. In this study we processed the GPS data of three annual campaigns from years 2003–2008 using Bernese 5.0 GPS software. The results were analysed based on the time series of baseline lengths and their temporal variation. On the average the length of a baseline varied less than 2.0 mm without any evident trend. Estimated velocities were small (0.2 mm/a) and mostly statistically insignificant because of the relatively short time series. More measurement campaigns are anticipated in the future to better constrain the limits for the deformation in the area, but it is not necessary to carry out measurements as frequently.*

*Key words: GeoSatakunta, GPS processing, crustal deformation*

### *1. Introduction*

The Finnish Geodetic Institute (FGI), the Geological Survey of Finland (GSF), Posiva Oy and municipalities in the district of Satakunta launched the GeoSatakunta research program in 2002 to carry out interdisciplinary studies on the regional bedrock stress field and to apply the results, e.g., in land use planning in the Satakunta area.

The bedrock in the Satakunta area offers exceptional possibilities for the stress field study. The structure and geological evolution of the area is well-known (Paulamäki *et al.*, 2002). It is characterised by younger bedrock units like Rapakivi bodies, Jotnian sandstone and olivine diabases, which cause marked changes in the stress field through variations in densities and structural properties (Huhta and Korsman, 2005). On the other hand, the bedrock experiences a postglacial uplift, about 6–7 mm/a (Mäkinen *et al.*, 2003). The uplift rate changes about 1 mm/a from NW to SE, which should cause some effect over time on the stress field of the crust. In addition, there are other processes listed in (Lambeck and Purcell, 2003), which can contribute to the regional stress field, like spreading of the Atlantic seafloor and its push against the Fennoscandian shield.

As a part of a larger co-operation project we established a regional GPS network in 2002 to obtain information about contemporary crustal deformation. Geodetic GPS measurements are the most accurate method to determine horizontal movements over a large area. Following the Olkiluoto deformation studies (*Kallio et al.*, 2009) we can achieve a detection threshold of 0.2 mm/a for single-site motion from ten years time series.

The aim of this study is to carry out a preliminary deformation analysis using the GPS data from years 2003-2008 and to determine the need for a follow-up study. In this paper we introduce the GeoSatakunta GPS network, discuss the GPS processing strategy and present the results of the time series analysis.

In addition to the GPS measurements presented here, there exist also other geodetic data in the area. These include repeated precise levelling (*Lehmuskoski et al.*, 2008), uplift values (*Mäkinen et al.*, 2003), gravimetric data (*Kiviniemi*, 1980; *Kääriäinen and Mäkinen*, 1997), and time series in the Olkiluoto area (*Chen and Kakkuri*, 1995; *Kallio et al.*, 2009; *Lehmuskoski*, 2008). We will not discuss them here.

## 2. Network and measurements

The GeoSatakunta GPS network has been established in two stages. The first pillars were built in 2002 in the vicinity of the city of Pori, and the network was later (2005–2006) expanded southwards, when the city of Rauma joined the project (*Poutanen and Ahola*, 2010). The network consists of 13 pillars and of the Olkiluoto permanent GPS station. The site selection was based on geological considerations by the Geological Survey of Finland, and the baseline lengths range from five to 65 km (Fig. 1).

The GPS pillars are made of reinforced concrete on-site. All the pillars are attached to the solid bedrock with iron bars. An antenna platform was installed on the top of the pillar at the same time the pillar was casted. The platform is made of stainless steel with a 5/8 inch hole in the middle to use a standard-sized bolt for the antenna. The antenna is directly attached to the platform without any interface or forced centring device, hence its height and position is preserved between campaigns (Fig. 2). We expect that the pillars are stable and the possible movements we observe are due to deformation. To control the stability of the pillars we established auxiliary markers at pillars in 2006 for repeated centring measurements.

We have carried out a total of 18 campaigns since January 2003 (three campaigns annually) using Ashtech Z12 and  $\mu$ Z dual frequency receivers and Ashtech Dorne Margolin Choke Ring antennas. The same antenna has been set up on the same pillar every time to eliminate the individual antenna phase centre errors. With 24 hour-long observation sessions we try to diminish or eliminate satellite geometry and signal multipath related errors. The campaigns were also performed at the same time every year to minimize any seasonal effects which are visible, e.g., in the Olkiluoto data (*Kallio et al.*, 2009).

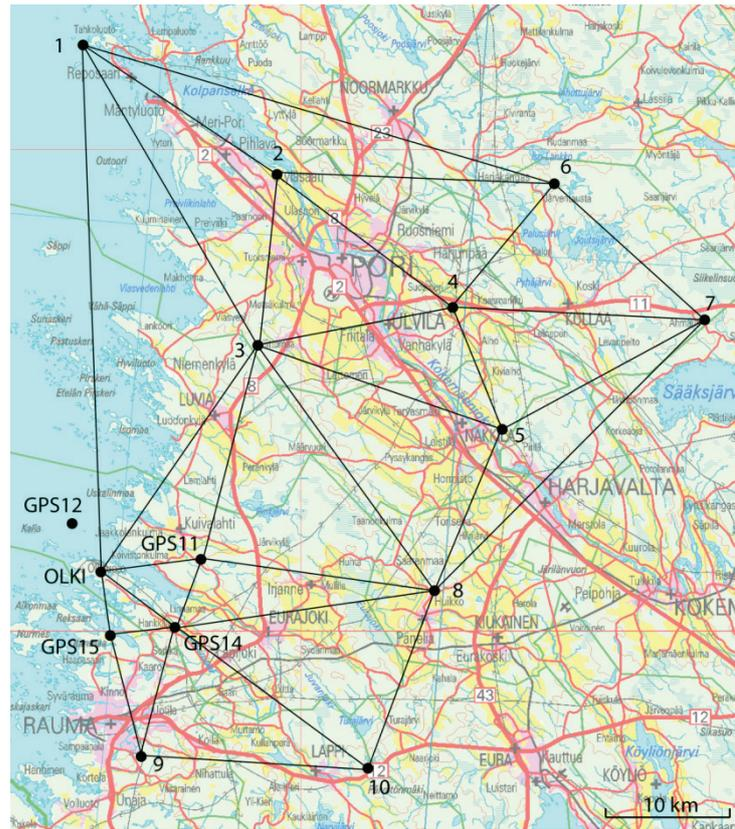


Fig. 1. GeoSatakunta GPS network.  
Base map © National Land Survey, license number 51/MML/09.



Fig. 2. GPS observations at Taipalmäki (GPS15), (photo Joel Ahola).

### 3. *GPS processing*

The computation was carried out using Bernese 5.0 software (*Dach et al., 2007*). The computation process was automated using the Bernese Processing Engine to process all campaigns in a reasonable time, which also enables a fast repeat of processing for developing and testing the computation strategy and parameters. The preliminary computation carried out after each measurement campaign revealed some outlying sessions and pillars with large scatter (*Poutanen and Ahola, 2010*). Hence, particular attention was given to the outlier detection to get a more reliable analysis from relatively short time series. We also applied correction tables from the individual absolute calibration of antennas, which were not available at the time of the preliminary computations.

The data processing strategy was based on the double-difference approach. We first computed entire set of baselines in each session. After that a network adjustment was applied, where the Olkiluoto permanent station was kept fixed. As a result we obtained coordinates of the pillars for each campaign.

Single baselines were resolved in three stages. First we used the L3 ionosphere-free linear combination for data screening and outlier detection. The outlying solutions were removed automatically. The ambiguity resolution was carried out using the Quasi-ionosphere free combination (QIF) of the Bernese software (*Dach et al., 2007*), where both L1 and L2 observables are processed. Stochastic ionosphere parameters were estimated to reduce the influence of the ionosphere refraction and thus, to reach sufficiently good initial values for ambiguities. The final solution was estimated using the L3 and the resolved ambiguities. The elevation cut-off angle was set to 15 degrees, and the Niell troposphere model was adopted.

The rms-values of individual baselines varied from 0.5 to 1.6 mm. The residual screening did not affect the best resolved baseline (smallest rms-values), but generally it slightly improved the solutions. In the case of problematic observation sites and sessions, the rms-values decreased after the residual screening to the same order of magnitude as in the other vectors.

### 4. *Analysis*

The coordinate time series were analysed in two parts. First, we briefly introduce and discuss the time series of the baseline lengths and compare the results with the preliminary computation (*Poutanen and Ahola, 2010*). Second, we perform a simple deformation analysis to determine the velocities for the pillars and to obtain the first approximation of the crustal movements.

#### 4.1 *Baseline length time series*

We computed baseline lengths from the adjusted coordinates of the pillars. The main features of the time series are presented in Figures 3–5. The results of the preliminary computation (*Poutanen and Ahola, 2010*) were also included for

comparison. On the average the baseline length in 18 campaigns varied less than 2.0 mm, and the session-to-session scatter was in the most cases smaller than in the preliminary computation. The largest scatter was observed at baselines from the site 5, where obstacles are limiting the visibility. However, the difference to the other sites is not as large as in preliminary computation. In addition, a large scatter was detected at the site 8, but the reason for that is not as obvious.

The baseline length time series from a single station to all other stations behave fairly uniformly, although we could not observe seasonal variation like in the Olkiluoto network (*Kallio et al.*, 2009). The detected behaviour is partly due to the uniform processing of the data. Other major causes probably arise from the unique measurement conditions in every session and the related atmospheric modelling. For any further interpretation, a more thorough error analysis is needed.

The standard deviations as a function of baseline length (Fig. 4) show no outlying observations, and the small distance dependency is as expected. Thus, none of the observation sites is significantly more uncertain than the others indicating a successful outlier rejection during the data processing. However, a few outlying sessions remain in the baseline length time series despite the successful GPS processing (Fig. 5).

The detection threshold for statistically significant movement depends on the length of time series, number of sessions and the variance of lengths. With these time series the limit is relatively high compared to the size of deformations that might be expected in this area. In a few cases the scatter is as low as 1.0 mm, but longer time series are needed to achieve the corresponding detection level.

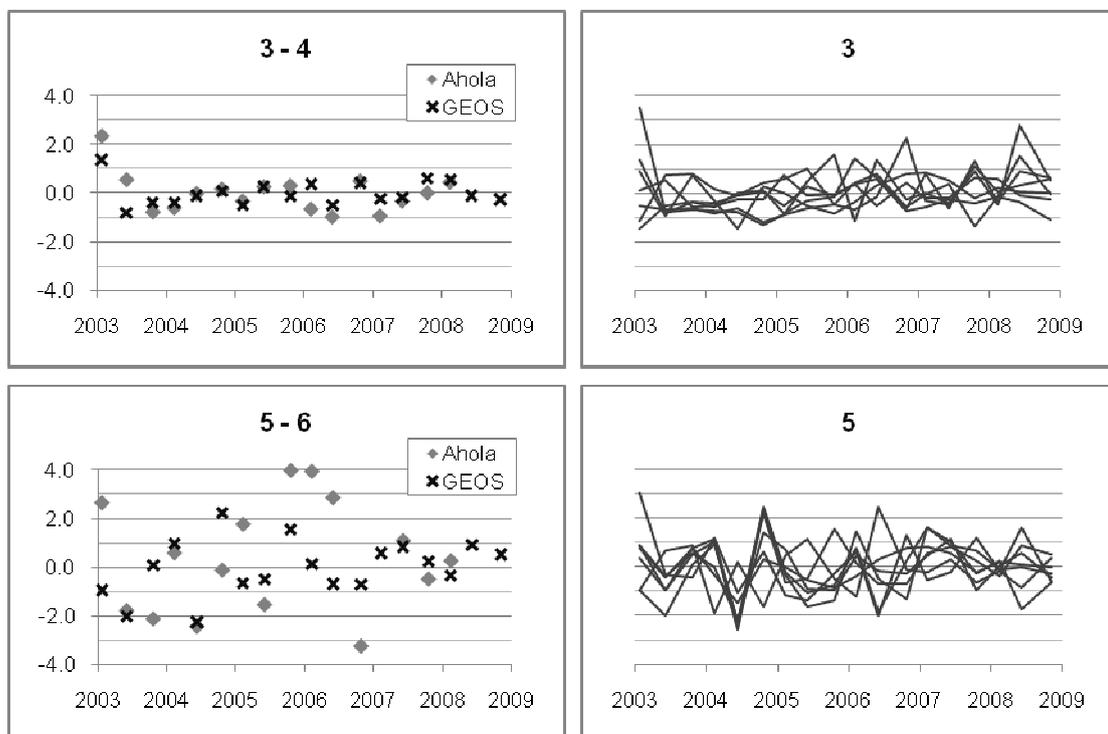


Fig. 3. Example of a good (3–4) and a problematic baseline (5–6), deviation from mean in millimetres. Label Ahola refers to the preliminary computation (*Poutanen and Ahola*, 2010), label GEOS to this determination. All baseline lengths from points 3 and 5 are shown at right.

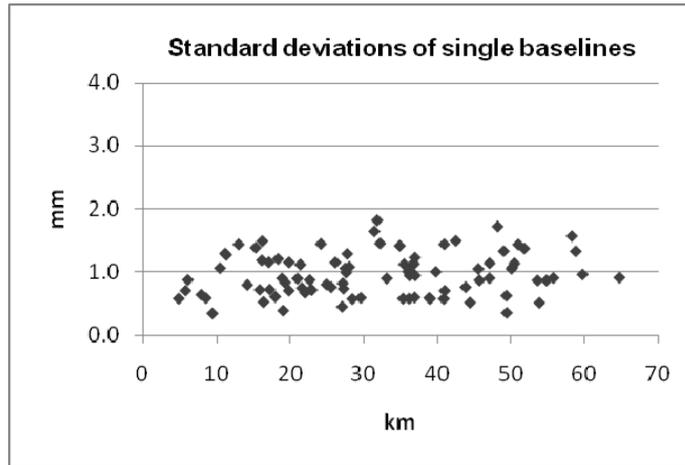


Fig. 4. Standard deviation of baselines as a function of the baseline length.

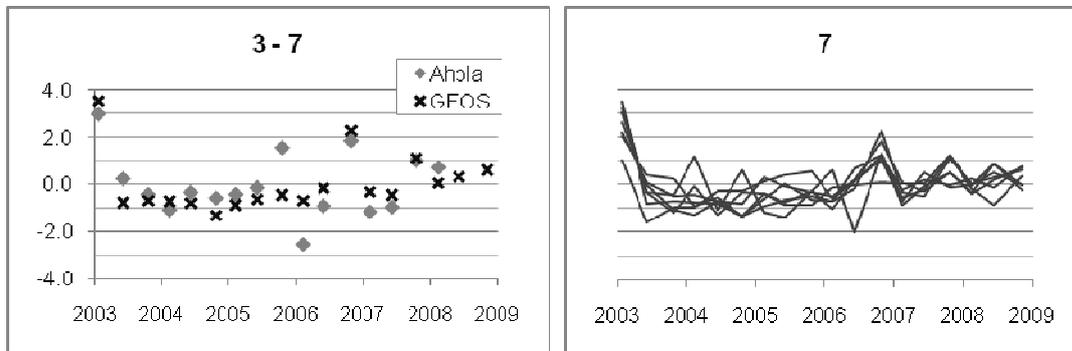


Fig. 5. The results of a few campaigns (e.g., 2003-1 and 2006-3 at site 7) deviate from all other sessions although GPS-observations were screened during the processing.

#### 4.2 Horizontal velocities

The deformation analysis was based on the coordinate differences between adjacent pillars, which were determined automatically using Delaunay-triangulation. A free network adjustment was applied with station specific velocity parameters ( $v_x$ ,  $v_y$ ,  $v_z$ ) as additional parameters. Because we had no fixed reference coordinates or velocities, there exists a rank deficiency in the normal equation matrix. The solution of unknown parameters was reached by using the pseudoinverse of the normal matrix. In the process the sum of the velocities remains zero. The resolved velocities were transformed to the North-East-Up system. We used a  $3\sigma$  criterion to test the statistical significance of the estimated velocities, which corresponds roughly the 99 % confidence level.

In the first approach the deformation analysis was performed for the entire network. The results show that only the north component of the pillar 6 is statistically significant (Table 1). The larger standard deviations of the southern part of the network are due to the shorter time series. Our tests showed that minor changes in GPS processing strategy affected the magnitudes and directions of the velocity vectors, although the alternative GPS solution was nearly as good as the final one. Hence the estimated velocities, especially for the southern part of the network, are uncertain.

In the second approach the deformation analysis was performed using only the northern pillars (1–7) and the Olkiluoto station, which have longer and therefore more reliable time series. The results of the first campaign (2003-1) were omitted from the analysis, because the results deviate from all other campaigns. The results are presented in Table 2. To illustrate the results the station velocities were interpolated in a grid and plotted as a velocity vector field (Fig. 6).

Now we could estimate statistically significant velocities for pillars 3, 6 and 7. The estimated velocities are small (max 0.2 mm/a) but of the same order of magnitude as in Olkiluoto deformation studies (e.g. *Kallio et al.*, 2009). The standard deviations are slightly smaller than in the first analysis for the entire dataset. In addition the solution is not as sensitive to the GPS-processing strategy as in the first estimate. When overlaying the vectors with the geological information the possible change seems to take place in the vicinity of geologically interesting features, like the major shear zones and the Jotnian sandstone. More observations are needed to confirm the results.

Table 1. Results of the deformation analysis (statistically significant velocities in bold).

	North		East	
	[mm/a]		[mm/a]	
	Velocity	St.dev	Velocity	St.dev
<b>1</b>	-0.10	0.08	0.03	0.06
<b>2</b>	0.12	0.08	0.11	0.06
<b>3</b>	-0.13	0.07	0.03	0.05
<b>4</b>	-0.11	0.08	0.05	0.06
<b>5</b>	0.11	0.08	0.16	0.06
<b>6</b>	<b>0.32</b>	0.08	0.15	0.06
<b>7</b>	0.00	0.08	0.11	0.06
<b>8</b>	0.18	0.23	0.19	0.16
<b>9</b>	0.24	0.15	-0.23	0.11
<b>10</b>	0.18	0.19	-0.38	0.13
<b>11</b>	-0.22	0.14	-0.13	0.10
<b>14</b>	-0.30	0.14	-0.04	0.10
<b>15</b>	-0.31	0.18	-0.14	0.13
<b>OLKI</b>	0.01	0.07	0.08	0.05

Table 2. Results of the deformation analysis for the subnet with the longest time series (statistically significant velocities in bold).

	North [mm/a]		East [mm/a]	
	Velocity	St.dev	Velocity	St.dev
<b>1</b>	-0.08	0.07	-0.07	0.05
<b>2</b>	0.03	0.07	-0.06	0.04
<b>3</b>	-0.17	0.06	<b>-0.13</b>	0.04
<b>4</b>	-0.13	0.06	-0.02	0.04
<b>5</b>	0.04	0.07	0.07	0.04
<b>6</b>	<b>0.24</b>	0.07	0.04	0.05
<b>7</b>	0.00	0.08	<b>0.17</b>	0.05
<b>OLKI</b>	0.06	0.08	0.01	0.05

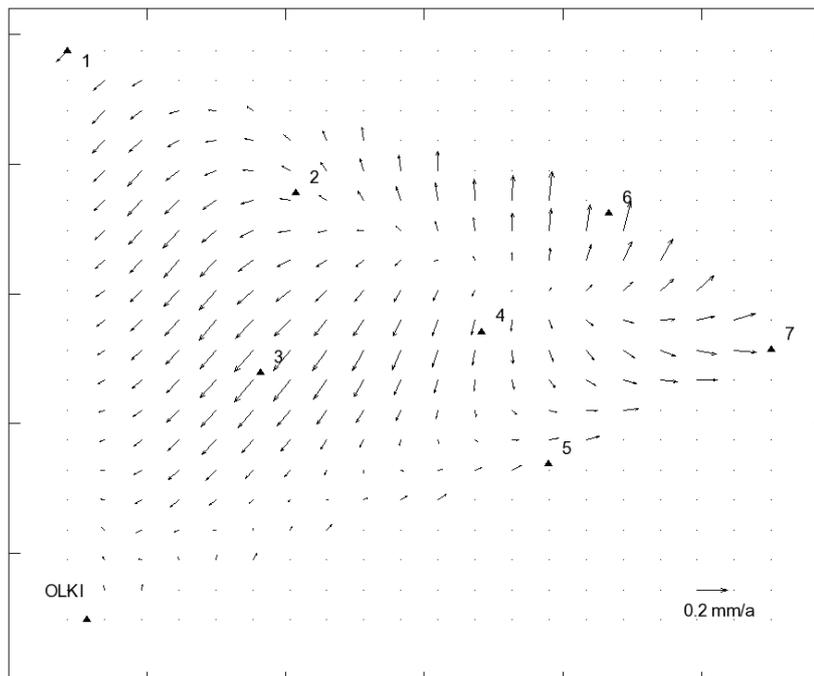


Fig. 6. The interpolated velocities presented as a vector field for the northern part of the network. The uncertainties of the velocities are on the average 0.07 and 0.05 mm/a in the N and E components, respectively.

Table 3. Simulated standard deviations of the coordinates and velocities. A 1 mm standard error was used for the coordinate differences in the simulation.

	<b>Coord st.dev x3 [mm]</b>	<b>Velocity st.dev x3 [mm/a]</b>
<b>1</b>	0.60	0.11
<b>2</b>	0.63	0.11
<b>3</b>	0.50	0.08
<b>4</b>	0.56	0.10
<b>5</b>	0.55	0.10
<b>6</b>	0.63	0.11
<b>7</b>	0.61	0.10
<b>8</b>	1.05	0.15
<b>9</b>	0.93	0.15
<b>10</b>	0.98	0.14
<b>11</b>	0.84	0.13
<b>14</b>	0.87	0.13
<b>15</b>	1.12	0.17
<b>OLKI</b>	0.53	0.09

## 5. *Conclusions and future*

On the basis of six years of measurements we have achieved a detection threshold of 0.3 mm/a for single-site motion. Using the subnet with the longest history the threshold diminishes to about 0.2 and 0.1 mm/a in the N and E components, respectively. A more sophisticated statistical analysis is needed to draw any definite conclusions about motions, as well as longer time series.

We plan to continue our activities in the area also in the future. By using the same model as in the deformation analysis above one can simulate how the accuracy will improve in coming years. We should detect velocities less than 0.15 mm on a 99 % confidence level, when continuing observations once a year during 2010–2014 (Table 3).

GPS observing campaigns in the network, combined with the activity at the Olkiluoto, will be the basis of the upcoming research. We also plan to use existing gravity data and GPS-levelling results to compute a local geoid model, to fit it better in the sharp geoid features at the River Kokemäki. The Satakunta network is the first high-precision network in Finland of this size, and therefore, a valuable test field for geodetic techniques to detect minor deformations and network stability.

### *Acknowledgements*

*The Cities of Pori and Rauma* are acknowledged for building the GPS observation pillars and helping us during the measurement campaigns. We would also like to thank Maaria Nordman, Jyrki Puupponen and Pasi Häkli for carrying out measurement campaigns. This project was partly funded by Satakuntaliitto (European Union/ Aluekehitysrachasto) and Academy of Finland, project RCD-Lito, 122822.

### *References*

- Chen, R. and J. Kakkuri, 1995. GPS work at Olkiluoto for the year 1994. *Posiva Work Report PATU-95-30e*, Posiva Oy, Helsinki.
- Dach, R., U. Hugentobler, P. Fridez and M. Meindl, 2007. Bernese GPS Software, Version 5.0. Astronomical Institute, University of Bern.
- Huhta, P. and K. Korsman, 2005. Bedrock Stress Field in the Satakunta Region. *Geological Survey of Finland*, Report P 34.4.042
- Kääriäinen, J. and J. Mäkinen, 1997. The 1979-1996 gravity survey and the results of the gravity survey of Finland 1945-1996. Kirkkonummi.
- Kallio, U., J. Ahola, H. Koivula, J. Jokela and M. Poutanen, 2009. GPS Operations at Olkiluoto, Kivetty and Romuvaara in 2008. *Posiva Working Report 2009-75*. POSIVA Oy, Olkiluoto.
- Kiviniemi, A., 1980. Gravity Measurements in 1961-1978 and the Results of the Gravity Survey of Finland in 1945-1978. Helsinki.
- Lambeck, K. and A. Purcell, 2003. Glacial Rebound and Crustal Stress in Finland. *Report 2003-10*. POSIVA Oy.
- Lehmuskoski, P., 2008. Precise Levelling of the Olkiluoto GPS Network in 2007. *Working Report 2008-19*. POSIVA Oy, Olkiluoto.
- Lehmuskoski P., V. Saaranen, M. Takalo and P. Rouhiainen, 2008. Suomen Kolmannen tarkkavaaituksen kiintopisteluettelo. Bench Mark List of the Third Levelling of Finland. *Publications of the Finnish Geodetic Institute* No. **139**. Kirkkonummi, 220 p.
- Mäkinen, J., H. Koivula, M. Poutanen and V. Saaranen, 2003. Vertical Velocities in Finland from Permanent GPS Networks and from Repeated Precise Levelling. *Journal of Geodynamics*, Vol 35:4-5, 443-456.
- Paulamäki, S., M. Paananen and E. Elo, 2002. Structure and geological evolution of the bedrock of southern Satakunta, SW Finland. *Posiva Report*, 2002-04.
- Poutanen, M and J. Ahola, 2010. Maankuoren liiketutkimukset Satakunnassa GPS-mittausten avulla. *To be published in "Geotietoa Satakunnasta. Geo-Satakunta ja InnoGeo-projektien loppuraportti"*, (The final report of the collaboration projects GeoSatakunta and InnoGeo) Report Series of the Geological Survey of Finland. (In Finnish)